analytical chemistry

Technical Note

pubs.acs.org/ac

Colony Lysate Arrays for Proteomic Profiling of Drug-Tolerant Persisters of Cancer Cell

Kohei Kume[†,§] and Satoshi S. Nishizuka[*,†,‡]

[†]Division of Biomedical Research and Development, Institute of Biomedical Science, Iwate Medical University, Morioka, Iwate 020-8505, Japan

[‡]Center for Applied Proteomics and Molecular Medicine, Institute for Advanced Biomedical Research, George Mason University, Manassas, Virginia 20110, United States

Supporting Information

ABSTRACT: Functional heterogeneity of cancer cells is one of the key properties to understanding relapse after drug treatment. Hence, clarification is needed with regard to which types of subgroups of cancer cells dominantly contribute to the initiation of relapse. Recently, we established the colony lysate array (CoLA), which is a method that allows comparison of individual colonies at the protein level to assess the initiation of anticancer drug-tolerant persisters (DTPs) based on the reverse-phase protein array (RPPA) system. DTPs grow in various drug concentrations and types showing 2-dimensional growth (~1 mm) on a flat surface. The size of DTPs are larger than spheroids (~0.3 mm) in agarose gel, which makes them easy to handle for a number of assays. DTPs provide functional information during the process of their formation, initiating from the origin of a drug-tolerant single cell. Using >2000 DTPs generated from various drugs and doses profiled on the basis of 44 proteins, we demonstrate that the DTPs are clustered on the basis of their proteomic profiles changing in response to drugs and doses. Of interest, nine transcription factors in the DTPs, such as STAT3 and OCT4A, were identified as having decreased or increased levels of proteins in response to gefitinib. Importantly, these results can be obtained only by individual proteomic colony profiling, which may identify alternative therapeutic targets and biomarkers for DTPs that may harbor critical mechanisms for cancer relapse.

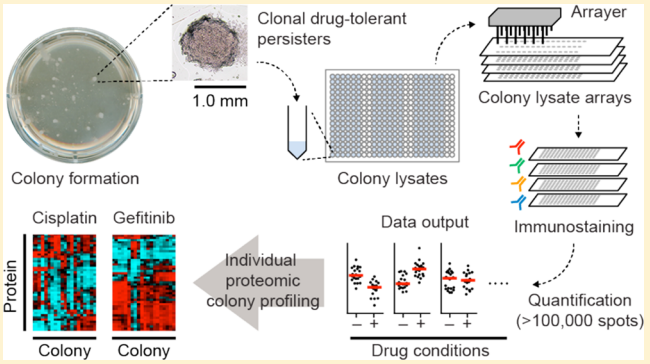

One of the major problems with current cancer treatments is relapse after chemotherapy. Most relapses occur within five years after chemotherapy of advanced solid tumors, while the acquisition of genetic alterations during de novo cancer development requires more than 10 years.[1,2] This fact indicates that nongenetic mechanisms may be underlying the chemoresistance. Previous investigations have suggested that cellular and clonal heterogeneity could be induced by mechanisms distinct from genetic heterogeneity, which contribute to the protection of the cancer cell population from potentially lethal drug exposure both in vitro and in vivo.[3,4] Therefore, relapse initiation should occur from subpopulations that are capable of proliferating under the presence of drugs in the heterogenic population. However, a very limited number of technologies has been available to date for profiling such individual small populations. Therefore, the technical development of methods that can monitor changes at the protein level in heterogeneous clones is urgently needed for understanding the mechanisms of cancer relapse.

Recently, we introduced the colony lysate array (CoLA) method for quantitatively measuring protein levels of individual colonies based on the reverse-phase protein array (RPPA) system.[5] On the basis of the idea that colony formation in the presence of anticancer drugs resembles relapse after chemotherapy in humans, we investigated colony-forming drug-tolerant persisters (DTPs)[3] induced by different types of cells grown under several drug conditions, using the CoLAs. Hierarchical clustering of the quantitative CoLA data identified stemness- and epithelial-dominant clusters based on the proteomic profile of individual colony-forming DTPs.[5] However, the levels of protein markers between individual colony-forming DTPs were highly heterogeneous, suggesting that DTPs are more stochastically, rather than deterministically, emerged populations. These findings finally led to the discovery of a combinatorial strategy using α-amanitin and cisplatin (CIS) for the prevention of *peritonitis carcinomatosa*.[5]

Here, we describe a technique for colony lysate collection followed by CoLA data analysis. Drug concentrations applied for DTP isolation are started from the 50% colony inhibitory concentration (CoI_{50}) unique to the drug and cells, with five 10-fold dilution series. The colony is defined as a 1 mm in diameter cell cluster (approximately 1.0×10^4 cells), and the

Received: April 1, 2017
Accepted: July 28, 2017
Published: July 28, 2017

DOI: 10.1021/acs.analchem.7b01215
Anal. Chem. 2017, 89, 8626−8631

lysates are collected with manual pipetting. The resulting colony-derived lysates were printed on a nitrocellulose membrane in a high-density (7 dots/mm^2) format. Hierarchical clustering as well as principal component analysis (PCA) for identifying functionally relevant subpopulations are highlighted as two examples of CoLA analysis.

EXPERIMENTAL SECTION

Sample Preparation. The CoI_{50} values of CIS, docetaxel (DTX), gefitinib (GEF), and sorafenib (SOR) against human cancer cells, including HCT116, HeLa, HT29, MCF7, and MKN45, were first determined by a conventional 24-well plate format colony formation assay. For colony lysate collection, cells were plated in a 6-well plate in 10-fold serial dilutions of a drug starting from the CoI_{50} value. Single colonies were picked up with a pipet tip and lysed in 10 μL of Pink Buffer (PB; 9 M urea, 4% CHAPS, 65 mM DTT, 2% Pharmalyte).[6] The advantages of PB usage have been described elsewhere.[6,7] Briefly, this buffer maintains high concentrations of denatured proteins without heat. The lysed product was subjected to a high-speed centrifugation (14 000g). The resulting lysate supernatant (~8 μL) was transferred to another microtube while avoiding aspiration of the remaining precipitate (~2 μL). The colony lysate was then plated in a set of conical 384-well microplates (Genetix, New Milton, Hampshire, UK) based on an array design described below.

Colony Formation Assays. Two-dimensional (2D) colony formation assays with MKN45 and HeLa.S-Fucci2 cells were performed as previously described.[5] The 3D colony formation (soft agar) assay with MKN45 cells was performed using a slight modification of a previously described method.[8] Briefly, 1.0×10^3 cells were suspended in 500 μL of 0.33% agarose in RPMI1640 medium containing 10% fetal bovine serum and plated on top of 1 mL of 0.55% agarose in the same medium in a well of a six-well culture plate. Plates were incubated for 21 days at 37 °C with 5% CO_2 in a humidified incubator. For immunocytochemistry, 2D colonies were fixed and stained in the culture dishes as previously described.[5] The 3D colonies in agarose were picked up with microtweezers, and more than 100 colonies were pooled in a 1.5 mL centrifuge tube containing 1.0 mL of phosphate buffered saline. Pooled colonies were then fixed in 4% paraformaldehyde for 15 min at room temperature, embedded in paraffin, and sectioned at a 5 μm thickness. Immunocytochemistry was performed with either mouse anti-c-MYC (9E10, Santa Cruz Biotechnology, Santa Cruz, CA) or rabbit anti-c-MYC (D84C12, Cell Signaling Technology, Danvers, MA, USA) antibodies according to the manufacturer's protocol. Secondary antibodies were CF488A-conjugated antimouse or CF594-conjugated antirabbit antibodies (Biotinum, Hayward, CA, USA). The nuclei were stained with Hoechst 33342 or 4′6-diamidino-2-phenylindole (DAPI) (Dojindo Laboratories, Kumamoto, Japan). Images were collected on an IN Cell Analyzer 2000 automated microscope or BX43 fluorescent microscope (Olympus, Tokyo, Japan). The fluorescence images were false-colored in green or blue using Photoshop CS5 version 12.0.4 (Adobe, San Jose, CA).

CoLA. CoLA configurations consisted of 2400 lysates in a 17.2 × 22.4 mm^2 area with a 115 μm pin diameter and a 450 μm dot-to-dot pitch. For CoLA printing, an Aushon Biosystems 2470 Arrayer and its graphical user interface were used (Aushon Biosystems, Billerica, MA, USA) to print the lysate onto nitrocellulose-coated glass slides (Grace BioLabs, Bend, OR, USA). The number of depositions per feature was set to 5. A representative CoLA slide from a batch production was stained by colloidal gold (Bio-Rad, Hercules, CA, USA). The estimated total protein amount attached on the surface was between 0.1 and 0.5 ng. The total protein content was used to adjust antibody signals. CoLAs were then individually stained with 44 prescreened primary antibodies[5] followed by colorimetric detection using a catalyzed signal amplification (CSA) system with diaminobenzidine (DAB; Dako Japan, Tokyo, Japan). The set of primary antibodies was selected to assess the involvement of stemness, pluripotency, epithelial mesenchymal transition, cell cycle, apoptosis, cell structure, autophagy, and adhesion in the context of drug resistance (Table S1). Both signal levels from colloidal gold and DAB were obtained using the reflective mode of an optical flatbed GT-X970 scanner (EPSON, Suwa, Japan) and then converted into raw pixel values using P-SCAN[9] or WinPscan software with 8-bit gradation and 1200 dpi resolution (http://www.nishizukalab.org/downloads-2). Respective resulting matrices were used for downstream analysis.

Data Analysis and Visualization. The spot signal matrices were normalized by $\log_2$ transformation of raw intensity data. The antibody signal from each spot was adjusted by subtracting the corresponding total protein value. Adjusted values were then subtracted by the row and column mean. Each mean-subtracted column value was divided by the standard deviation. The resulting protein × colony matrix was visualized by a heatmap with an average-linkage hierarchical clustering using CIMminer (https://discover.nci.nih.gov/cimminer/home.do).[10] To validate the CIM patterns in CIS- and GEF-induced clusters, the protein × colony matrices were also visualized by PCA scores plot using JMP version 9.0 (SAS Institute, Cary, NC, USA). A PCA loadings plot for GEF-induced DTPs was performed to identify the transcription factors that had increased or decreased levels in a dose-dependent fashion from the 44 proteins tested. One-way analysis of variance (ANOVA) was performed using GraphPad Prism version 7.02 (GraphPad Software, La Jolla, CA).

RESULTS AND DISCUSSION

The Smallest Unit To Profile Functional Cancer Cell Subpopulations. Historically, the body of molecular knowledge of tumor cells has been obtained from cells in bulk. However, tumors are generally an aggregation of numerous individual cells that have genetic and functional heterogeneity. Therefore, the smallest unit within a tumor to profile should be an individual cell. Recent observations have already demonstrated genetic heterogeneity of individual tumor cells from various tumor types.[11,12] In the context of drug resistance, functional heterogeneity is the most crucial factor for understanding the mechanism. The drug-resistant phenotype can be reversible, develops in a relatively prompt manner, and evolves as the tumor grows.[3,4] Hence, the profiling method for functional heterogeneity can only be assessed in cells that have the ability to continuously divide in the presence of drugs at the initiation stage of their development. Overall, the smallest unit for profiling cancer cell subpopulations in drug resistance studies is the colony-forming DTPs that can divide in the presence of drugs. Several technologies have been developed to analyze such a small unit of the heterogeneous cell population (Table S2). Flow cytometry (FCM) is one of the most widely used techniques to characterize individual cells in a given population based on cellular markers. Information from FCM may be interpreted with respect to minor cell subpopulations

DOI: 10.1021/acs.analchem.7b01215
Anal. Chem. 2017, 89, 8626−8631

and enables subsequent functional analysis for the isolated cell subpopulation.[13] A fluorescence-based cytometric system can count cells "as is" but only allows for the simultaneous detection of fewer than 10 proteins.[14] Another format of FCM that enhances the multiplex detection ability, mass cytometry (MCM), has also been developed and offers detection of >40 simultaneous cellular parameters at single cell resolution.[15,16] Among cell lysate-based techniques, a special form of Western blot, namely, single-cell Western blot (scWB), can multiplex protein targets and constitutes a versatile tool for protein detection at single cell resolution.[17,18] Recent advances in single-cell reverse transcription PCR (scRT-qPCR) and RNA sequencing (RNA-seq) allow for the quantification of >300 or >100 000 transcripts from a single cell, respectively.[19,20] However, these techniques are very costly for analyzing a large number of subclones to characterize drug-resistant cells. To date, immunohistochemistry (IHC) and image cytometer (ICM) have been considered to be optimal methods for molecularly profiling the smallest functional units, such as DTPs, but with limited multiplexity due to the requirement of fluorescent-based systems for simultaneous detection.[21,22] In contrast to the above techniques targeting single cells, CoLA is designed to profile colony-forming DTPs with a panel of proteins, which are functional cancer cell populations capable of propagating in the presence of drugs.[3]

Use of 2D Colonies. There are two types of colonies based on growth support in vitro, two-dimensional (2D) and three-dimensional (3D) colonies (i.e., spheroids), that grow in various drug conditions.[3,23] The 2D colonies are feasible to handle and grow in cultures with only attachment to the bottom surface of a plate coated by materials such as vacuum-gas plasma-treated or fibronectin-coated polystyrene, which has been widely used in conventional colony formation assays.[24] In contrast, 3D colonies can be obtained from culture medium that supports cell attachment from multiple dimensions with agar, agarose, and methylcellulose.[25,26] Both types of colonies are hypothesized to have a relatively homogeneous genetic background, since they initiate from a single cell and represent subpopulations that promptly adapt to drug stress.[3,23] The major apparent difference between 2D and 3D colonies is the size, which directly affects the feasibility of handling them during experimental manipulation. The 2D colonies are generally 1 mm in diameter and contain up to 10 000 cells (~13−14 cell divisions),[5] whereas the diameter of 3D spheroids is generally between 50 and 200 μm and comprised of up to 100 cells (~6−7 cell divisions).[25,27] The size of 3D colonies limits the ability of visual confirmation and manual handling for single colony manipulation (Figure 1). In addition, 3D colonies seem to bear some functional differences from 2D colonies in terms of drug sensitivity[28] and may be more appropriate than individual colony profiling when assessing cellular matrix function.[22] A previous report used bulk 3D colonies that emerged from stressed culture conditions for proteomic analysis with RPPA;[23] however, this study was not directly designed to investigate the heterogeneity among clones. Nevertheless, the data from bulk 3D colonies still provided some unique findings.

To confirm the utility of 2D colonies in functional profiling, fluorescent immunocytochemistry was performed in both 2D and 3D colonies. The c-MYC protein, as a transcription factor, is regulated by multiple upstream signaling pathways to promote cancer cell survival and proliferation.[29] From a therapeutic viewpoint, it has been shown that c-MYC plays a

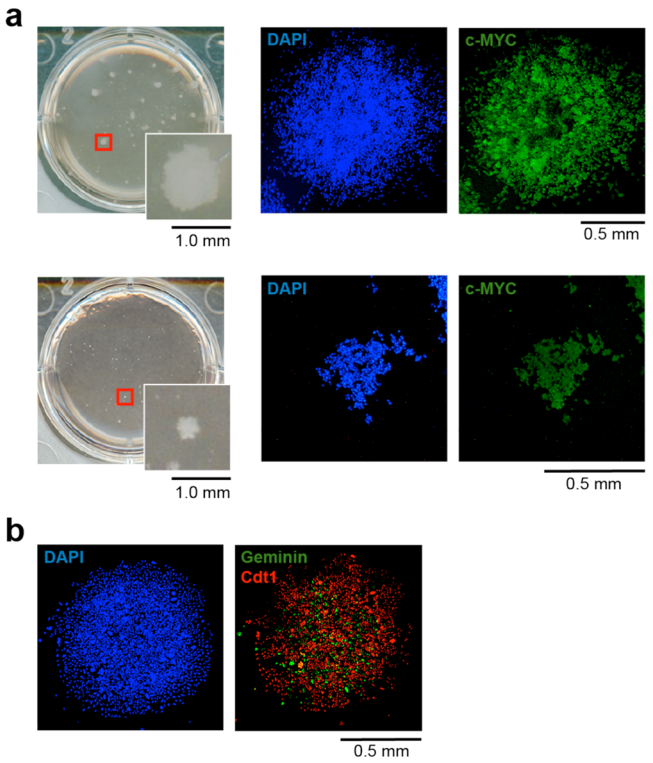

Figure 1. Comparison of 2D and 3D colonies grown in a 6-well plate for 13 d. (a) A representative 2D (top) or 3D (bottom) colony stained with anti-c-MYC antibody (green) and DAPI (blue). (b) Intracolony heterogeneity of HeLa cells in terms of Geminin. Fluorescent images of a representative HeLa.S-Fucci2 colony expressing mCherry-hCdt1 (red) and mVenus-hGeminin (green) are shown. DAPI (blue) was used to stain nuclear DNA.

critical role in the transcriptional regulation of therapeutic-resistant cells.[30−32] The c-MYC protein showed relatively homogeneous expression in individual colony-forming cells in both 2D and 3D colonies, indicating that 2D colonies could be equally informative in function to 3D colonies (Figure 1a). Using the fluorescence ubiquitination cell cycle indicator (Fucchi) system, we found that some proteins, such as cell cycle-related Geminin, may not be entirely homogeneous (e.g., synchronized) in a 2D colony (Figure 1b). However, the advantage of 2D colonies in visualization and handling provides large-scale functional subpopulation profiling in cancer cells. The estimated protein yield from each lysate generated from a 2D colony with a diameter of 1 mm was as low as 0.2 mg/mL in 10 μL of lysate (i.e., 2 μg). Using our CoLA procedure, the one dot per single colony printing configuration accommodated >700 dots/cm^2. With this high-density colony representation, CoLA allows for the profiling of >3800 colonies per experiment across many proteins with our current configurations.

CoLA Production and Validation. DTPs derived from 5 cell lines (HCT116, HeLa, HT29, MCF7, and MKN45) grown in the presence of 6 serial dilutions of 4 drugs (CIS, DTX, GEF, and SOR) were collected. Holding the micropipette as shown in Figure S1a, the colony picking takes approximately 7 s per colony. During this step, a 1 mm diameter colony was scraped with the pipet tip to converge to one end point and aspirated immediately after the last stroke (Figure S1b). When the colony was aspirated with approximately 5 μL of medium, the colony was generally drawn up to the top surface of the inner medium and then the inner medium could be dispensed,

DOI: 10.1021/acs.analchem.7b01215
Anal. Chem. 2017, 89, 8626−8631

leaving approximately 1 μL of residual media containing a single colony (Figure S1c). A single colony with minimum medium can be dissolved in 10 μL of PB without any visible precipitate. Twenty biological replicates were obtained from each drug condition resulting in a set of 2400 colonies (Figure 2). Since the total protein concentration in each colony lysate

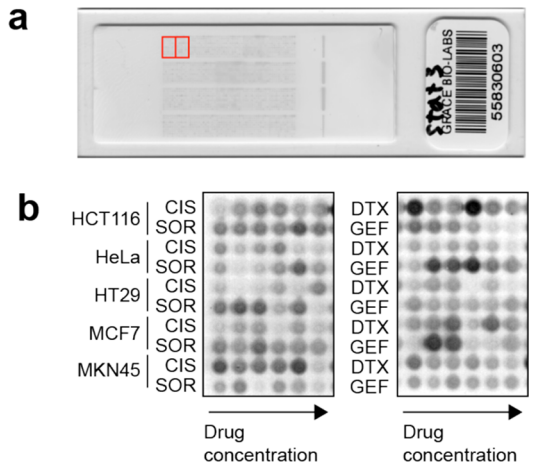

Figure 2. A representative immunostained CoLA. (a) A CoLA slide stained with a specific primary antibody for STAT3 using the CSA system. (b) A magnified view of the two red boxes in (a). These boxes contain a full set of lysates from individual colonies of cell lines with tested drug conditions. Twenty sets of biological replicates are accommodated on a slide.

was estimated to be 20% of cell lysates for a traditional RPPA, the number of depositions per feature was set to 5 (set to 1 for RPPA[33]). We did not use printing replicates because they were nearly identical to those from our quality control study.[33] Each CoLA was immunostained with one primary antibody. All antibody signals were quantified using P-SCAN or WinPscan, even though the signals appeared faint.[5] The image analysis of E-cadherin by WinPscan confirmed the positive correlation with CK8 (r = 0.86, P < 0.0001) and negative correlation with vimentin (r = −0.74, P < 0.0001), reflecting epithelial/nonepithelial protein relationships (Figure 3a). Interestingly, DTX-induced DTPs tend to show E-cadherin^{high}/CK-8^{high}, whereas molecular targeting drug (GEF and SOR)-induced DTPs closely distributed as E-cadherin^{low}/vimentin^{high} subpopulations. These data validate that the "biological integrity" of DTPs can be addressed in this experimental system.[34]

Proteomic Profiling of Colony-Forming DTPs. One-way ordered hierarchical clustering in terms of protein for each drug-by-drug dose allowed for the comparison of proteomic changes in response to the drug doses (Figure 3b). The cluster image map (CIM)[10] of the "CIS-induced cluster" demonstrated similar patterns between drug concentrations of 0 and 200 nM, suggesting that DTPs induced by CIS may have been able to tolerate drug-induced stress with a pre-existing population. In contrast, the GEF-induced cluster at 1 and 10 μM showed distinct patterns from those of lower concentrations. This observation suggests that DTPs induced by GEF reflect an adaptive response to the drug within small populations.[35] In a PCA scores plot, data points with respect to CIS clones were not discriminated by the CIS doses (Figure 3c), while those with respect to GEF doses showed a trend along the first principal component (PC1), explaining 49.9% of the variance (Figure 3d). The PCA loadings plot for GEF-induced DTPs

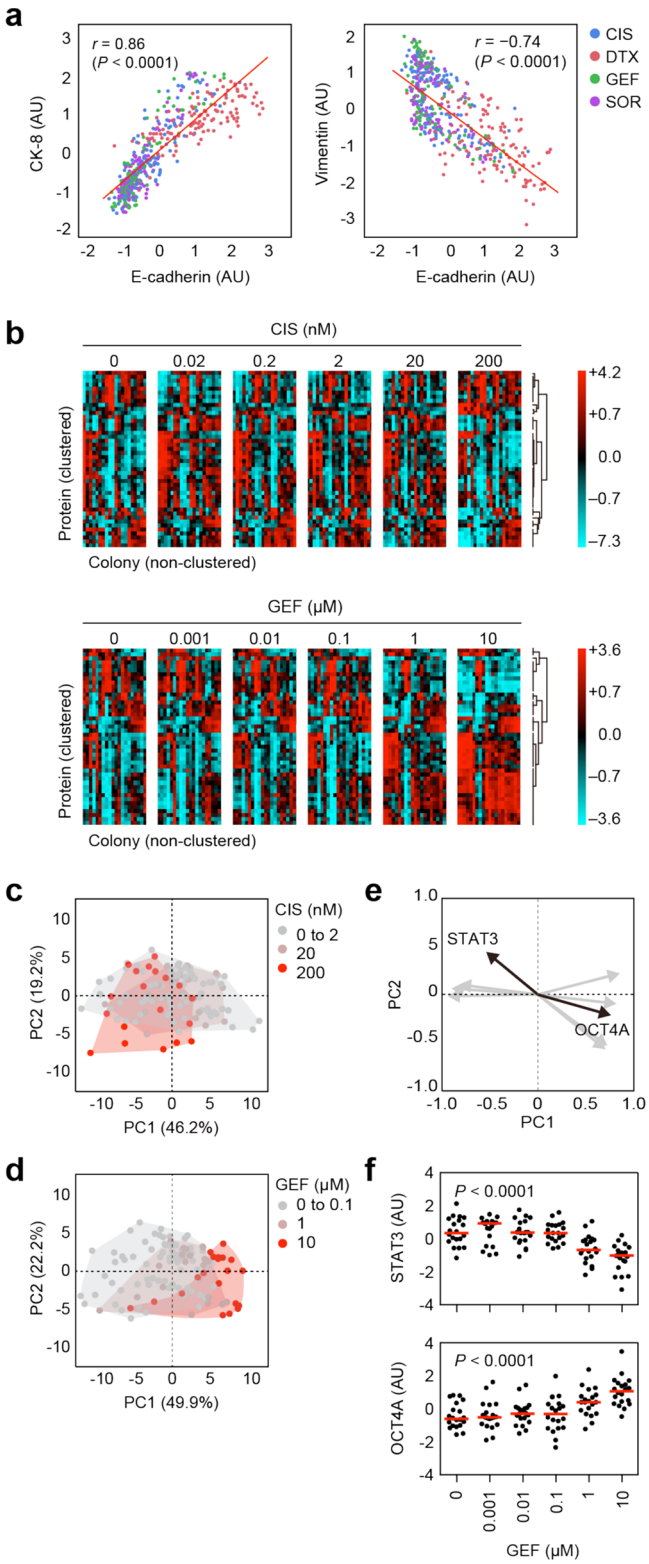

Figure 3. Visualization of CoLA data. (a) Correlation of epithelial (E-cadherin and CK-8) and mesenchymal (vimentin) markers in colony-forming DTPs of HCT116 from indicated drug conditions. Scatter plots of E-cadherin versus CK-8 or vimentin are shown with Pearson's correlation coefficient, r. (b) Comparison of the proteomic profiles across drug type and concentrations. One-way hierarchical clustering of proteins is shown on the vertical axis, and 20 colonies arranged in printed order (nonclustered) are shown on the horizontal axis. Validation of the CIM patterns in (c) CIS- and (d) GEF-induced clusters using a principal component analysis (PCA) scores plot with

DOI: 10.1021/acs.analchem.7b01215
Anal. Chem. 2017, 89, 8626−8631

Figure 3. continued

the first two principal components. Each data point representing individual colonies is colored according to the drug concentration. PC, principal component. (e) PCA loadings plot for GEF-induced DTPs illustrating the transcription factors that contribute strongly to the PC scores. Vectors indicate nine loadings of transcription factors plotted along negative or positive PC axes. (f) Dose responses of STAT3 and OCT4A levels in GEF-induced DTPs. Red lines indicate the median values of individual colonies for each condition. *P* values are of one-way ANOVA. CIS, cisplatin; GEF, gefitinib.

showed that nine transcription factors tested, such as STAT3 and OCT4A, were negatively or positively correlated along the PC axis, indicating their contribution to the PC scores (Figures 3e and S2). The GEF dose response of DTPs confirmed that the levels of STAT3 and OCT4A decreased and increased, respectively, in a dose-dependent manner (Figure 3e). The dose-dependent responses with these transcription factors support our previous study showing that the transcriptional machinery is well associated with the phenotype of colony-forming DTPs.[5] In our previous study, we found that an RNA polymerase II inhibitor, α-amanitin, restrains CIS-induced DTPs in vitro and in vivo. One of the therapeutic targets of α-amanitin is TAF15, which is involved in the RNA polymerase II transcriptional machinery.[5] Taken together, these results suggest that the drug-adaptive response of GEF-induced DTPs is due to transcriptional regulation. Although the distribution of CIS- and GEF-induced DTPs in terms of proteomic profile was different (Figure 3b–d), it may suggest that transcriptional machinery represents one of the critical mechanisms for acquisition of the drug-resistant phenotype.

CONCLUSIONS

An RPPA-modified method, CoLA, has been successfully established for individual proteomic colony profiling. Colony-forming DTPs are the smallest unit that can be designated as drug-resistant cells, and CoLA is one of the most suitable methods to profile DTPs at the protein level. Results of the validation studies suggest that CoLA can be used as a tool to understand the emergence mechanisms of DTPs from 2D colonies. With the molecular analysis of DTPs, CoLA offers an essential framework to identify molecular targets and reasonable drug combinations to suppress DTP propagation. The molecular characteristics of DTPs may reflect the entity of cancer cell subpopulations that dominantly contribute to postchemotherapeutic cancer relapse. At the preclinical level, CoLA will provide an alternative approach for understanding the mechanisms of cancer relapse.

ASSOCIATED CONTENT

Supporting Information

The Supporting Information is available free of charge on the ACS Publications website at DOI: 10.1021/acs.analchem.7b01215.

Colony picking method (Figure S1); PCA loadings plot with the two principal components for GEF-induced DTPs (Figure S2); primary antibodies (Table S1); analytical methods for the smallest unit molecular profiling of the heterogeneous cell subpopulation (Table S2) (PDF)

AUTHOR INFORMATION

Corresponding Author

*E-mail: snishizu@iwate-med.ac.jp.

ORCID

Kohei Kume: 0000-0003-2856-5970

Present Address

§K.K.: Department of Systems Biology, Beckman Research Institute of City of Hope, Monrovia, CA 91016.

Notes

The authors declare no competing financial interest.

ACKNOWLEDGMENTS

We thank Dr. Atsushi Miyawaki for providing HeLa.S-Fucci2 cells. This work was supported by a Grant-in-Aid for Young Scientists (B) for K.K. (JP25830121 and JP16K18458); Scientific Research (C) for S.S.N. (JP25462034); Scientific Research on Innovative Areas for S.S.N. (JP16H01578) of MEXT KAKENHI; Fund for the Promotion of Joint International Research (Fostering Joint International Research) for S.S.N (JP15KK0317). K.K. was supported by a research fund from The Japan Prize Foundation. K.K. and S.S.N. were supported by grants from Keiryokai Research Foundation Nos. Y118 and 131, respectively.

REFERENCES

(1) Jones, S.; Chen, W. D.; Parmigiani, G.; Diehl, F.; Beerenwinkel, N.; Antal, T.; Traulsen, A.; Nowak, M. A.; Siegel, C.; Velculescu, V. E.; Kinzler, K. W.; Vogelstein, B.; Willis, J.; Markowitz, S. D. *Proc. Natl. Acad. Sci. U. S. A.* **2008**, *105*, 4283–4288.

(2) Yachida, S.; Jones, S.; Bozic, I.; Antal, T.; Leary, R.; Fu, B.; Kamiyama, M.; Hruban, R. H.; Eshleman, J. R.; Nowak, M. A.; Velculescu, V. E.; Kinzler, K. W.; Vogelstein, B.; Iacobuzio-Donahue, C. A. *Nature* **2010**, *467*, 1114–1117.

(3) Sharma, S. V.; Lee, D. Y.; Li, B.; Quinlan, M. P.; Takahashi, F.; Maheswaran, S.; McDermott, U.; Azizian, N.; Zou, L.; Fischbach, M. A.; Wong, K. K.; Brandstetter, K.; Wittner, B.; Ramaswamy, S.; Classon, M.; Settleman, J. *Cell* **2010**, *141*, 69–80.

(4) Kreso, A.; O'Brien, C. A.; van Galen, P.; Gan, O. I.; Notta, F.; Brown, A. M.; Ng, K.; Ma, J.; Wienholds, E.; Dunant, C.; Pollett, A.; Gallinger, S.; McPherson, J.; Mullighan, C. G.; Shibata, D.; Dick, J. E. *Science* **2013**, *339*, 543–548.

(5) Kume, K.; Ikeda, M.; Miura, S.; Ito, K.; Sato, K. A.; Ohmori, Y.; Endo, F.; Katagiri, H.; Ishida, K.; Ito, C.; Iwaya, T.; Nishizuka, S. S. *Sci. Rep.* **2016**, *6*, 25895.

(6) Anderson, L.; Seilhamer, J. *Electrophoresis* **1997**, *18*, 533–537.

(7) Nishizuka, S.; Charboneau, L.; Young, L.; Major, S.; Reinhold, W. C.; Waltham, M.; Kouros-Mehr, H.; Bussey, K. J.; Lee, J. K.; Espina, V.; Munson, P. J.; Petricoin, E., 3rd; Liotta, L. A.; Weinstein, J. N. *Proc. Natl. Acad. Sci. U. S. A.* **2003**, *100*, 14229–14234.

(8) Wu, S. P.; Theodorescu, D.; Kerbel, R. S.; Willson, J. K.; Mulder, K. M.; Humphrey, L. E.; Brattain, M. G. *J. Cell Biol.* **1992**, *116*, 187–196.

(9) Carlisle, A. J.; Prabhu, V. V.; Elkahloun, A.; Hudson, J.; Trent, J. M.; Linehan, W. M.; Williams, E. D.; Emmert-Buck, M. R.; Liotta, L. A.; Munson, P. J.; Krizman, D. B. *Mol. Carcinog.* **2000**, *28*, 12–22.

(10) Weinstein, J. N.; Myers, T. G.; O'Connor, P. M.; Friend, S. H.; Fornace, A. J., Jr.; Kohn, K. W.; Fojo, T.; Bates, S. E.; Rubinstein, L. V.; Anderson, N. L.; Buolamwini, J. K.; van Osdol, W. W.; Monks, A. P.; Scudiero, D. A.; Sausville, E. A.; Zaharevitz, D. W.; Bunow, B.; Viswanadhan, V. N.; Johnson, G. S.; Wittes, R. E.; Paull, K. D. *Science* **1997**, *275*, 343–349.

(11) Navin, N. E. *Genome Biol.* **2014**, *15*, 452.

(12) McGranahan, N.; Swanton, C. *Cancer Cell* **2015**, *27*, 15–26.

(13) Al-Hajj, M.; Wicha, M. S.; Benito-Hernandez, A.; Morrison, S. J.; Clarke, M. F. *Proc. Natl. Acad. Sci. U. S. A.* **2003**, *100*, 3983–3988.

DOI: 10.1021/acs.analchem.7b01215
Anal. Chem. 2017, 89, 8626–8631

(14) Mittag, A.; Lenz, D.; Gerstner, A. O.; Sack, U.; Steinbrecher, M.; Koksch, M.; Raffael, A.; Bocsi, J.; Tarnok, A. *Cytometry, Part A* **2005**, *65A*, 103−115.
(15) Spitzer, M. H.; Nolan, G. P. *Cell* **2016**, *165*, 780−791.
(16) Bendall, S. C.; Simonds, E. F.; Qiu, P.; Amir, E.-a. D.; Krutzik, P. O.; Finck, R.; Bruggner, R. V.; Melamed, R.; Trejo, A.; Ornatsky, O. I.; Balderas, R. S.; Plevritis, S. K.; Sachs, K.; Pe'er, D.; Tanner, S. D.; Nolan, G. P. *Science* **2011**, *332*, 687−696.
(17) Kang, C. C.; Yamauchi, K. A.; Vlassakis, J.; Sinkala, E.; Duncombe, T. A.; Herr, A. E. *Nat. Protoc.* **2016**, *11*, 1508−1530.
(18) Hughes, A. J.; Spelke, D. P.; Xu, Z.; Kang, C. C.; Schaffer, D. V.; Herr, A. E. *Nat. Methods* **2014**, *11*, 749−755.
(19) White, A. K.; VanInsberghe, M.; Petriv, O. I.; Hamidi, M.; Sikorski, D.; Marra, M. A.; Piret, J.; Aparicio, S.; Hansen, C. L. *Proc. Natl. Acad. Sci. U. S. A.* **2011**, *108*, 13999−14004.
(20) Wu, A. R.; Neff, N. F.; Kalisky, T.; Dalerba, P.; Treutlein, B.; Rothenberg, M. E.; Mburu, F. M.; Mantalas, G. L.; Sim, S.; Clarke, M. F.; Quake, S. R. *Nat. Methods* **2014**, *11*, 41−46.
(21) Starkuviene, V.; Pepperkok, R. *Br. J. Pharmacol.* **2007**, *152*, 62−71.
(22) Smalley, K. S.; Haass, N. K.; Brafford, P. A.; Lioni, M.; Flaherty, K. T.; Herlyn, M. *Mol. Cancer Ther.* **2006**, *5*, 1136−1144.
(23) Muranen, T.; Selfors, L. M.; Worster, D. T.; Iwanicki, M. P.; Song, L.; Morales, F. C.; Gao, S.; Mills, G. B.; Brugge, J. S. *Cancer Cell* **2012**, *21*, 227−239.
(24) Franken, N. A.; Rodermond, H. M.; Stap, J.; Haveman, J.; van Bree, C. *Nat. Protoc.* **2006**, *1*, 2315−2319.
(25) Courtenay, V. D.; Selby, P. J.; Smith, I. E.; Mills, J.; Peckham, M. J. *Br. J. Cancer* **1978**, *38*, 77−81.
(26) Nakahata, T.; Spicer, S. S.; Cantey, J. R.; Ogawa, M. *Blood* **1982**, *60*, 352−361.
(27) Chambers, K. F.; Mosaad, E. M.; Russell, P. J.; Clements, J. A.; Doran, M. R. *PLoS One* **2014**, *9*, e111029.
(28) Bissell, M. J.; Kenny, P. A.; Radisky, D. C. *Cold Spring Harbor Symp. Quant. Biol.* **2005**, *70*, 343−356.
(29) Dang, C. V. *Cell* **2012**, *149*, 22−35.
(30) Green, A. R.; Aleskandarany, M. A.; Agarwal, D.; Elsheikh, S.; Nolan, C. C.; Diez-Rodriguez, M.; Macmillan, R. D.; Ball, G. R.; Caldas, C.; Madhusudan, S.; Ellis, I. O.; Rakha, E. A. *Br. J. Cancer* **2016**, *114*, 917−928.
(31) Shi, X.; Mihaylova, V. T.; Kuruvilla, L.; Chen, F.; Viviano, S.; Baldassarre, M.; Sperandio, D.; Martinez, R.; Yue, P.; Bates, J. G.; Breckenridge, D. G.; Schlessinger, J.; Turk, B. E.; Calderwood, D. A. *Proc. Natl. Acad. Sci. U. S. A.* **2016**, *113*, E4558−4566.
(32) Moyo, T. K.; Wilson, C. S.; Moore, D. J.; Eischen, C. M. *Oncogene* **2017**, DOI: 10.1038/onc.2017.95.
(33) Nishizuka, S.; Ramalingam, S.; Spurrier, B.; Washburn, F. L.; Krishna, R.; Honkanen, P.; Young, L.; Shimura, T.; Steeg, P. S.; Austin, J. *J. Proteome Res.* **2008**, *7*, 803−808.
(34) Singh, A.; Settleman, J. *Oncogene* **2010**, *29*, 4741−4751.
(35) Holohan, C.; Van Schaeybroeck, S.; Longley, D. B.; Johnston, P. G. *Nat. Rev. Cancer* **2013**, *13*, 714−726.

DOI: 10.1021/acs.analchem.7b01215
Anal. Chem. 2017, 89, 8626−8631